Electronic supplementary information for

Adaptive Responses of Sterically Confined Intramolecular Chalcogen Bonds

Karuthapandi Selvakumar[a*] and Harkesh B. Singh[b*]

Table of Contents **Page**

S1. Measurement of cone angle S2

S2. Computation of electrostatic surface potential S3

S3. Calculation of E_{IChB} for 2-substituted systems S4

S4. Computation of strain energy S8

S5. Calculation of E_{IChB} for 2,4-disubstituted systems S11

S6 Calculations of rotation barrier S14

S7 Computation of reaction coordinates for the hydrolysis of arylselenenyl bromide models **16b** and **22b** S15

S8 Dispersion contribution to E_{net} and E_{IChB} S17

S9 References S19

S1. Measurement of cone angles

The space filling model for the coordinates of 2-formyl-6-methylphenylselenenyl bromide was generated in ChemCraft software.[1] Then, dummies were introduced to calculate the cone angle. The positions of the dummies were adjusted to form a cone at the periphery of atoms forming the cone as in illustrated Figure S1.

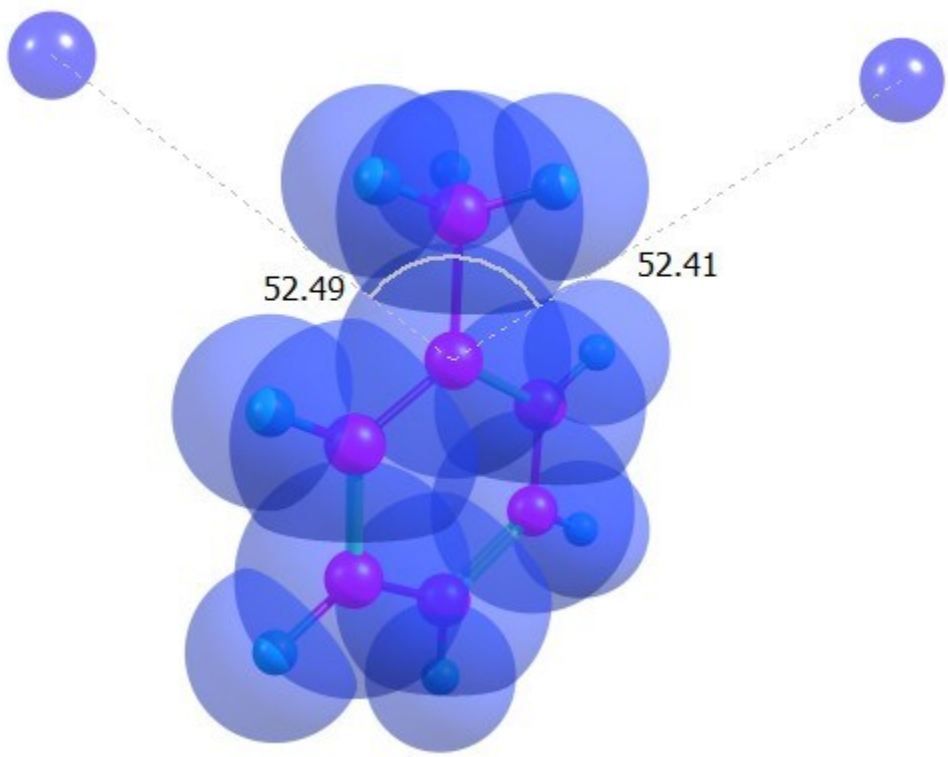

Figure S1. Showing the two half cone angles formed at the edges of van der Walls spheres of hydrogen atoms.

XYZ coordinates:

6	2.144500000	5.322800000	-0.001000000
6	2.136900000	3.822800000	0.000000000
6	3.404500000	3.083100000	0.000600000
6	3.398000000	1.750300000	0.000600000

6	2.122900000	1.022600000	0.000300000
6	0.971700000	1.694900000	0.000100000
6	0.979100000	3.162400000	-0.000100000
1	1.203600000	5.661400000	-0.001300000
1	2.617600000	5.653800000	-0.817500000
1	2.617300000	5.654800000	0.815300000
1	4.272900000	3.579000000	0.001000000
1	4.261500000	1.246000000	0.000900000
1	2.117900000	0.022600000	0.000100000
1	0.103200000	1.199200000	0.000100000
1	0.115600000	3.666900000	-0.000300000
0	-1.400600000	6.566900000	-0.000300000
0	3.337300000	6.654800000	3.455300000

S2. Computation of electrostatic surface potential (ESP)

All computational calculations were performed in Gaussian 09, Revision A.02.[2] The structures were optimized at B3LYP-D2/6-31g(d) level. The dispersion correction were requested using command iop(3/124=3). Atoms in molecules analysis (AIM)[3] were on these geometries using the key words #p B3LYP/6-311++G(2df,2p) iop(3/124=3) density=current output=wfn. The electrostatic potential (using file.wfn) were obtained using Multiwfn software,[4] and the pictures were drawn using VMD package.[5] ESPs were computed on isodensity surface, ρ(r)=0.001 au. Figure S2 shows the interaction of positive electrostatic potentials of "H" atom of formyl group in **9a**

with the negative electrostatic potential of "Se". Due to this interaction, "Se" of the "ArSe" do not have any blue color region (Negative ESP). Whereas "Se" of the "SeMe" has blue color regions.

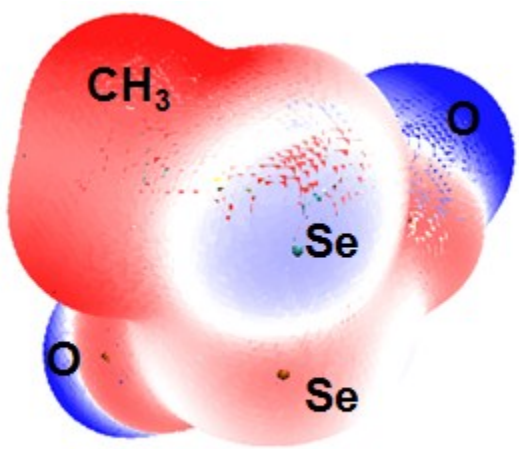

Figure S2. ESP map of **9a** (anti, anti) conformer showing the $H_{(CHO)}$···Se interaction, isodensity surface, ρ(r)=0.001 au.

S3. Calculation of E_{IChB} for 2-substituted systems

The structures of **2b**, **4b**, **8b**, **36** and **37** were optimized at B3LYP-D2/6-31g(d) level. The dispersion correction were requested using command iop(3/124=3). The key words used for this calculation is #p opt freq b3lyp/6-31g(d) iop(3/124=3). Computed structures do not have any imaginary frequencies. The IChB energy (E_{IChB} = ΔE) is the net energy of the homodesmic reaction (E_{IChB} = Sum of the product energy- Sum of reactant energy). The calculated electronic energies for the reactants and products are provides in Table S1 and computed E_{IChB} are provided in Table 2 of main manuscript..

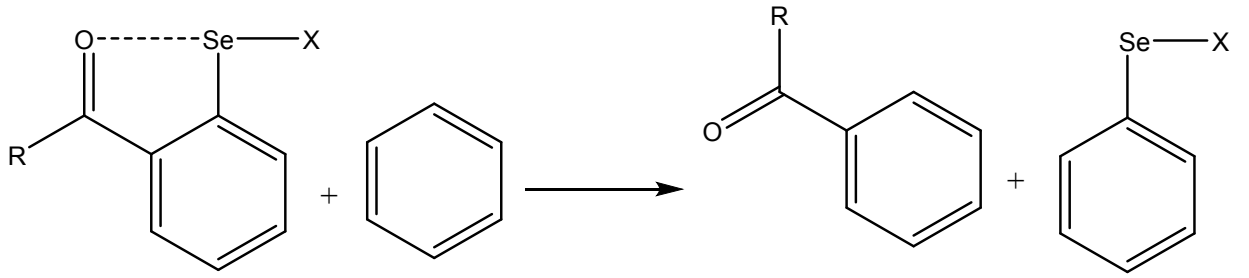

2b R = H, X=SeMe
8 R = H, X = Br
36 R= OMe, X = SeMe
37 R=OMe, X=Br

R = H or R = OMe

X= Br
or SeMe

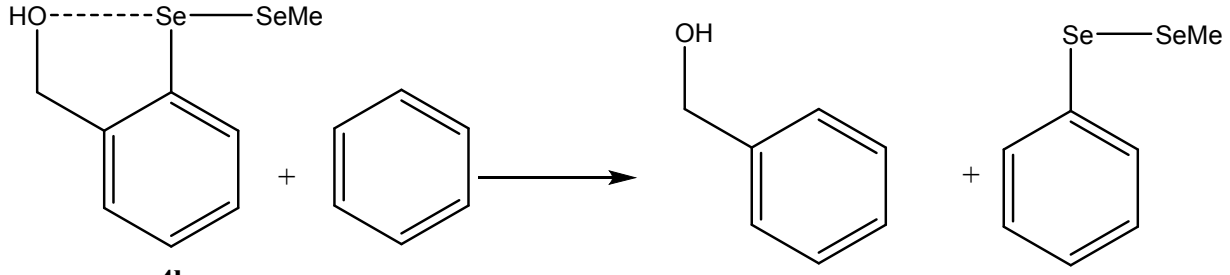

4b

Table S1.Provides the computed electronic energies of the reactant and products for homodesmic reactions of 2-substituted systems

Entry	**Energy** (Hartree)	**Entry**	**Energy** (Hartree)
PhCHO	-345.583824551	**2b**	-5183.69766908
PhCOOMe	-460.143180986	**4b**	-5184.89289257
Benzene	-232.255735693	**8**	-5316.1004815
$PhCH_2OH$	-346.780184001	**36**	-5298.25517387
PhSeBr	-5202.75998457	**37**	-5430.65692443
PhSeSeMe	-5070.36424726	-	-

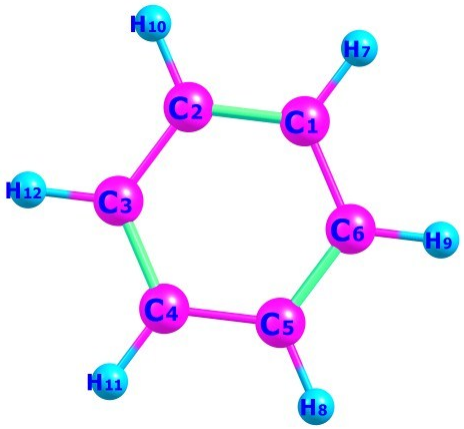

Benzene

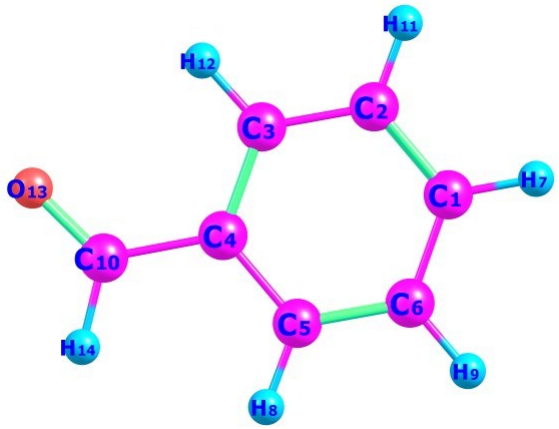

PhCHO

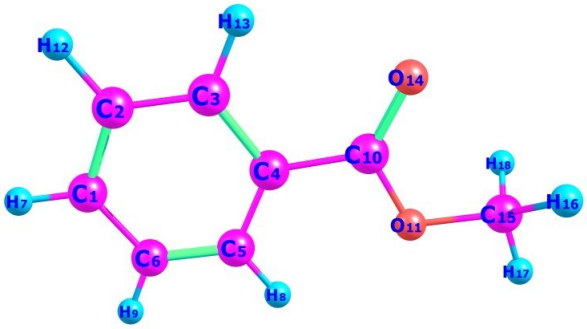

PhCOOMe

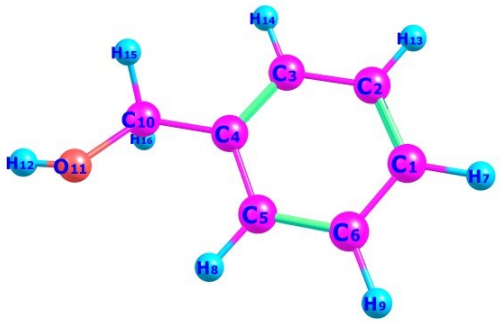

PhCH$_2$OH

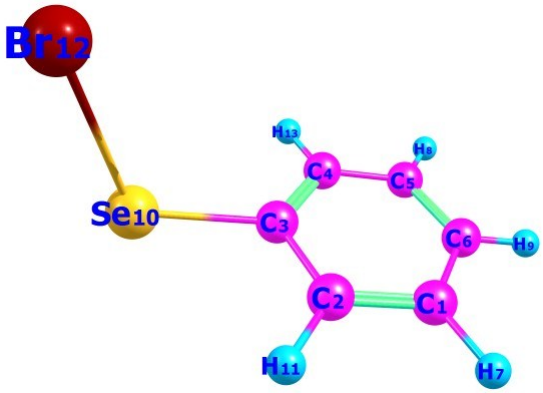

PhSeBr

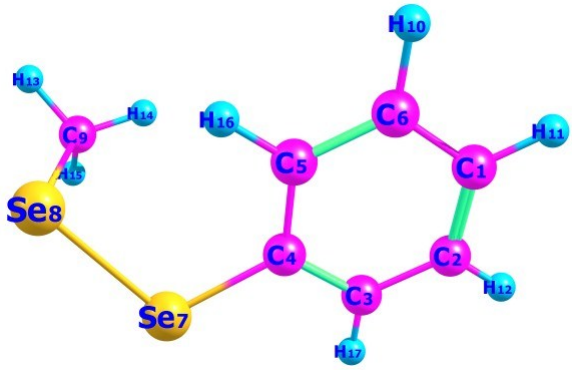

PhSeSeMe

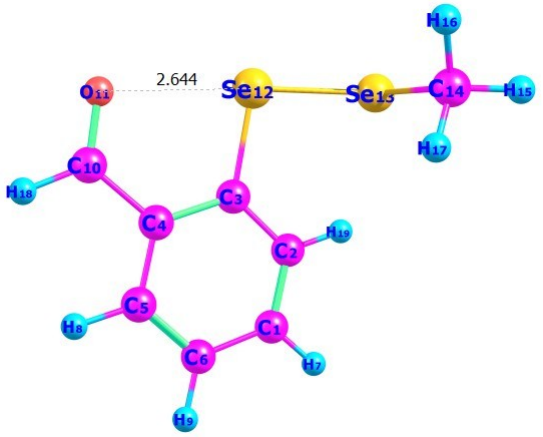
2.644
O11
Se12
Se13
C14
H16
H15
H17
C10
H18
C3
C4
C2
H19
C5
H8
C1
C6
H7
H9

2b

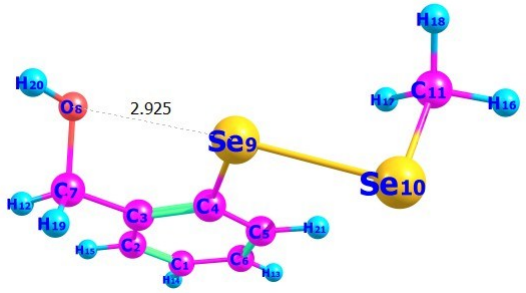
H18
H20
O8
2.925
C11
H17
H16
Se9
Se10
C7
H12
H19
C3
C4
C5
H21
H15
C2
C1
C6
H13
H14

4b

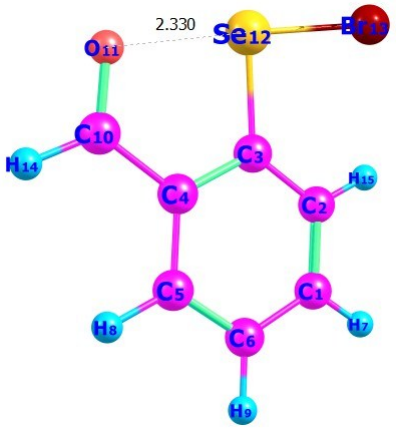
2.330
O11
Se12
Br13
C10
H14
C3
C4
C2
H15
C5
C1
H8
C6
H7
H9

8

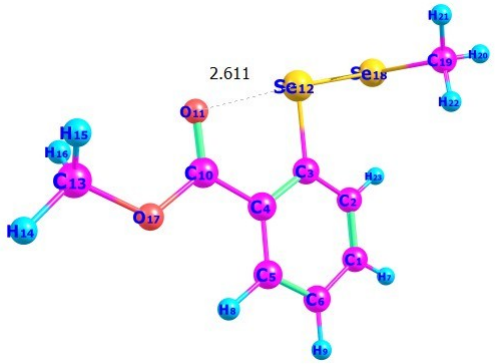
H21
2.611
Se12
Se18
C19
H20
O11
H22
H15
H16
C13
C10
C3
H23
C4
C2
H14
O17
C1
H7
C5
C6
H8
H9

36

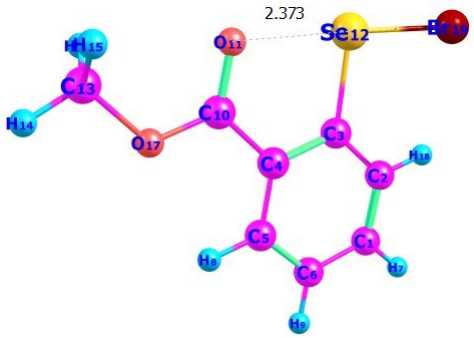
2.373
H15
O11
Se12
Br13
C13
H14
C10
O17
C3
C4
C2
H16
C5
C1
H8
C6
H7
H9

37

S4. Computation of strain energy

The structures of 2,6-disubstituted model systems X (**9b**, **10b**, **16b**, **17b**, and **22b**) and their 2,4-disubstituted isomers X′ (**9b′**, **10b′**, **16b′**, **17b′**, and **22b′**) were optimized at B3LYP-D2/6-31g(d) level. Computed structures do not have any imaginary frequencies. The energy difference between the two isomers is referred as the strain energy (E_{st} = Energy of the 2,4-disubstituted system - Energy of the 2,6-disubstituted system). The E_{st} are tabulated in Table S2.

Table S2. Provides the electronic energies of entries and the E_{st}

Entry	**Energy of X** (Hartree)	Entry	Energy X′ (Hartree)	**Est= ($E_{x'}$-E_x) × 627.509 (kcal/mol)**
9b	-5297.01548289	**9b′**	-5297.02499745	5.97
10b	-5526.13231653	**10b′**	-5526.1427186	6.53
16b	-5658.53065283	**16b′**	-5658.54399431	8.47
17b	-5299.42092146	**17b′**	-5299.41762039	-2.07
22b	-5429.41376412	**22b′**	-5429.4267831	8.17

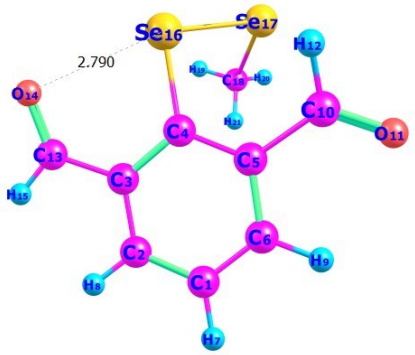

9b

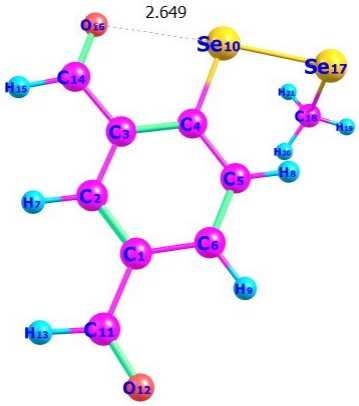

9b′

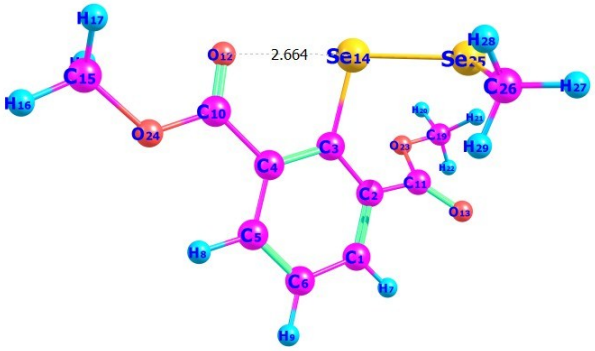

10b

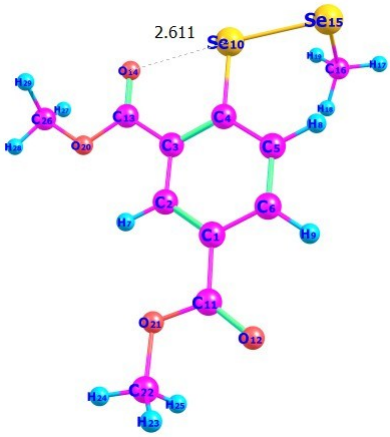

10b′

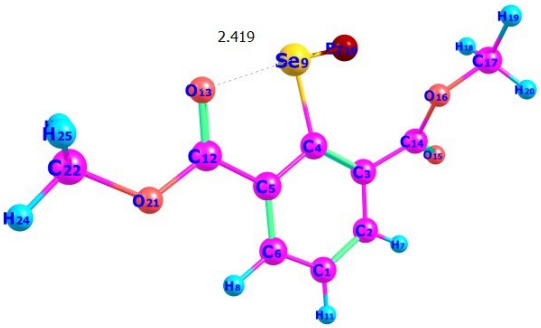

16b

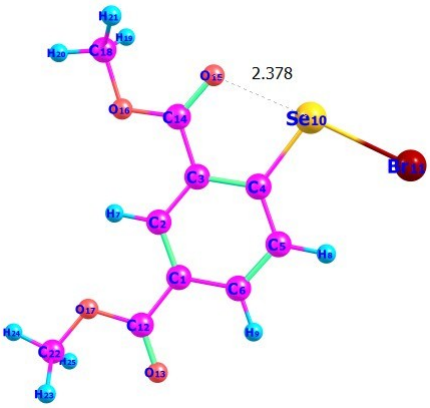

16b′

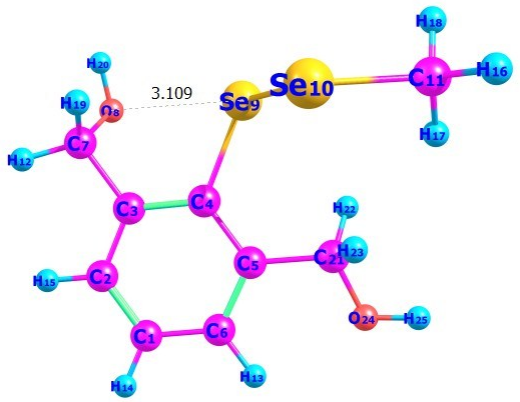

17b

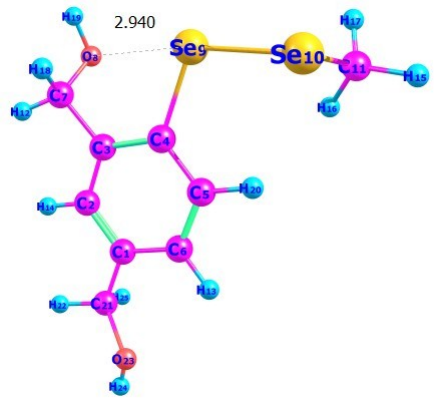

17b′

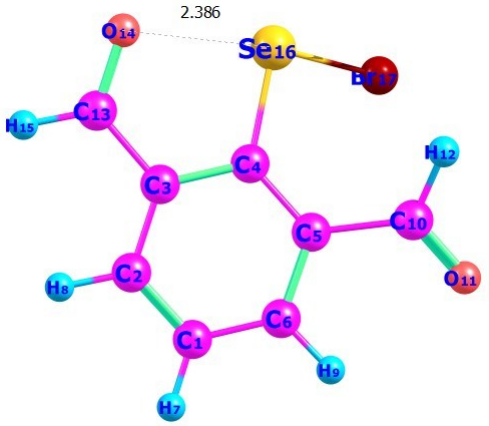

16b

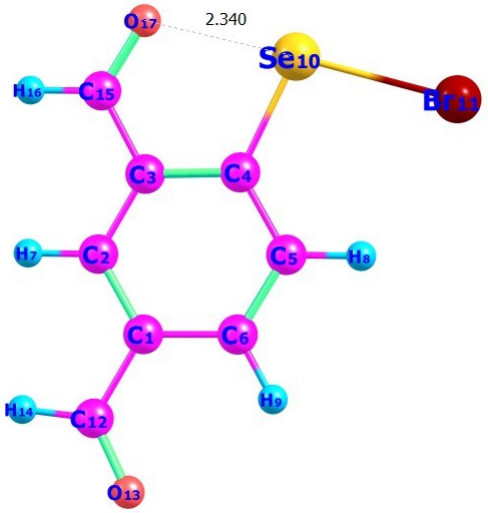

16b′

S5. Calculation of E_{IChB} for 2,4-disubstituted systems

Electronic energies of the 2,4-disubstituted isomers X′ (**9b′**, **10b′**, **16b′**, **17b′**, and **22b′**) and their homodesmic reaction partners and products were computed at B3LYP-D2/6-31g(d) level (Table S3). Computed structures do not have any imaginary frequencies. The E_{IChB} is the net energy of the homodesmic reaction (E_{IChB} = Sum of the product energy- Sum of reactant energy). The E_{IChB} are tabulated in Table 1 of the main manuscript.

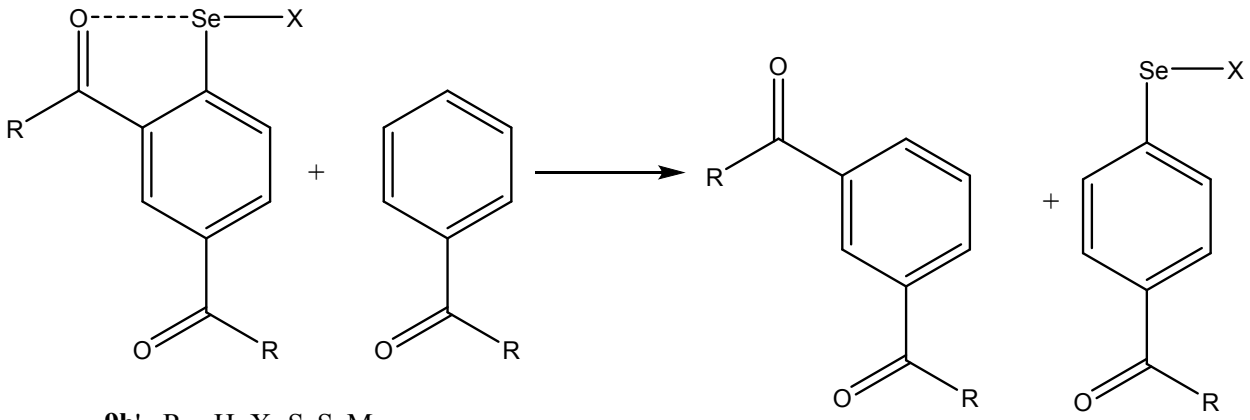

9b' R = H, X=SeSeMe
10b' R= OMe, X = SeSeMe
16b' R= OMe, X = Br
22b' R = H, X = Br

9b'' R = H, X=SeSeMe
10b'' R = OMe, X=SeSeMe
16b'' R=OMe, X=Br
22b'' R=H, X=Br

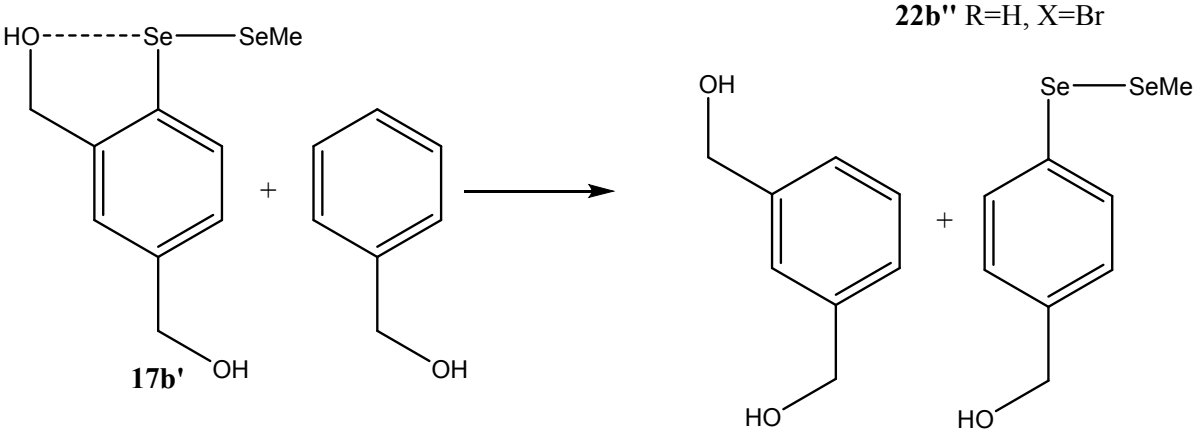

17b'

17b''

Table S3.Provides the sum of computed electronic energies the reactant and products of homodesmic reactions 2,4-disubstituted systems

Entry	Sum of reactant Energy (ΣE_R) (Hartree)	Sum of product Energy (ΣE_P) (Hartree)	$\Delta E=\Sigma E_P-\Sigma E_R$ (Hartree)	$\Delta E=\Sigma E_P-\Sigma E_R$ (kcal/mol)
9b′	-5642.608822	-5642.602998	-0.005824	-3.654328
10b′	-5986.285900	-5986.282224	-0.003675	-2.306341
16b′	-6118.687175	-6118.675536	-0.011639	-7.303735
17b′	-5646.197804	-5646.192202	-0.005602	-3.515433
22b′	-5775.010608	-5774.995449	-0.015159	-9.512464

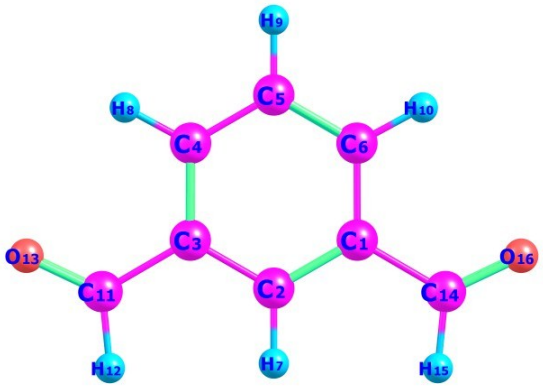

Isophthalaldehyde

Dimethyl isophthalate

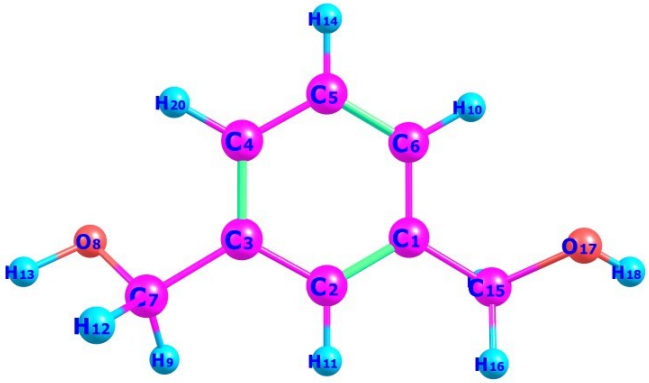

1,3-phenylenedimethanol

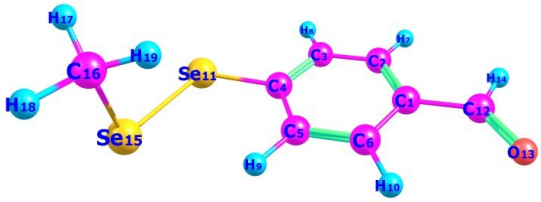

9b″

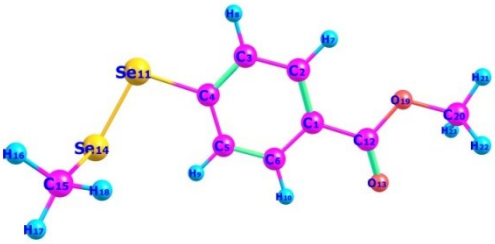

10b″

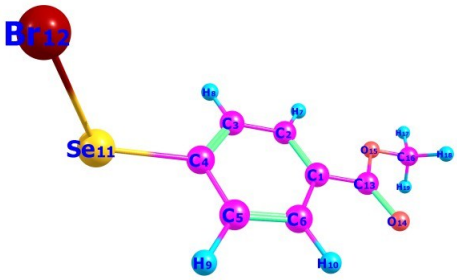

16b″

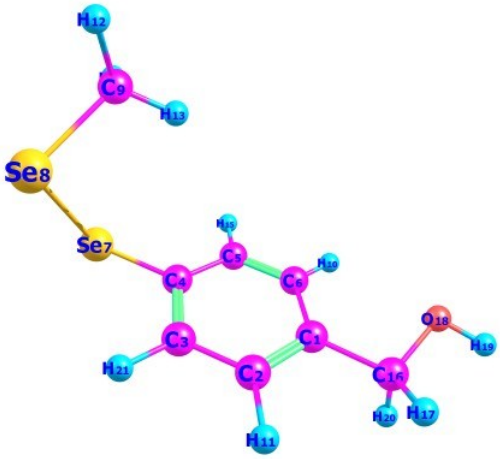

17b″

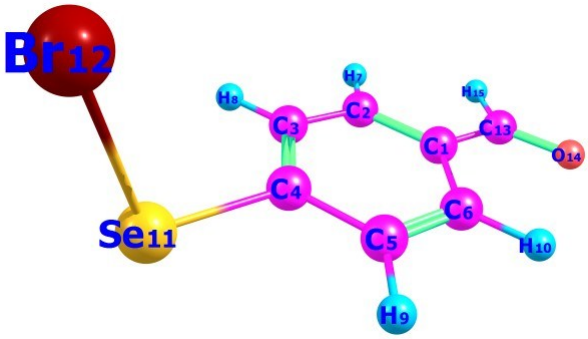

22b″

S6. Calculations of rotational energy barrier

The structures of benzaldehyde, methyl benzoate, and N-methylbenzamide systems were computed at B3LYP-D2/6-31 g(d) level. The one-dimensional potential energy surface was screened by rotating the carbonyl function around aryl plane. The keywords used for this calculation is #p opt=modredundant b3lyp/6-31g(d) iop(3/124=3). The functional groups (formyl, ester, and amide) were allowed to rotate around aryl plane and the energies were computed at every 10º interval of torsion angle. Then, the variation of electronic energy as a function of dihedral angle (=CH=CH-C=O) is plotted. Table S4 provides the rotational energy barriers.

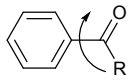

R = H, OMe, NHMe

Table S4. Shows the rotational energy barrier for the rotors

Entry	Energy Barrier (kcal/mol)
Benzaldehyde	9.847353
Methyl benzoate	7.560001
N-Methybenzamide	4.559326

S7. Computation of reaction coordinates for the hydrolysis of arylselenenyl bromides models 16b and 22b

The structures of reaction complexes (RC), transition states (TS), and the product complexes (PC) were optimized at B3LYP-D2/6-31 g(d) level. The frequency calculations indicates that the reactant complexes (**16-RC** and **22-RC**) and product complexes (**16b-PC** and **22b-PC**) does not show any imaginary frequencies. However, the transition states (**16b-TS** and **22b-TS**) showed one imaginary frequency along the reaction path. Table S5 provides the computed free energy along the reaction path.

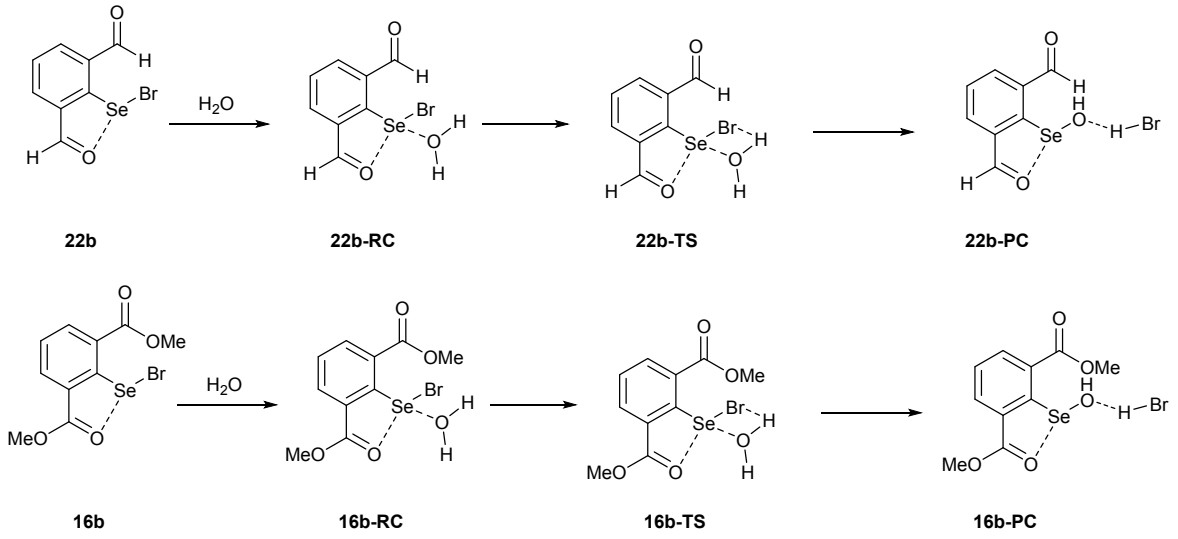

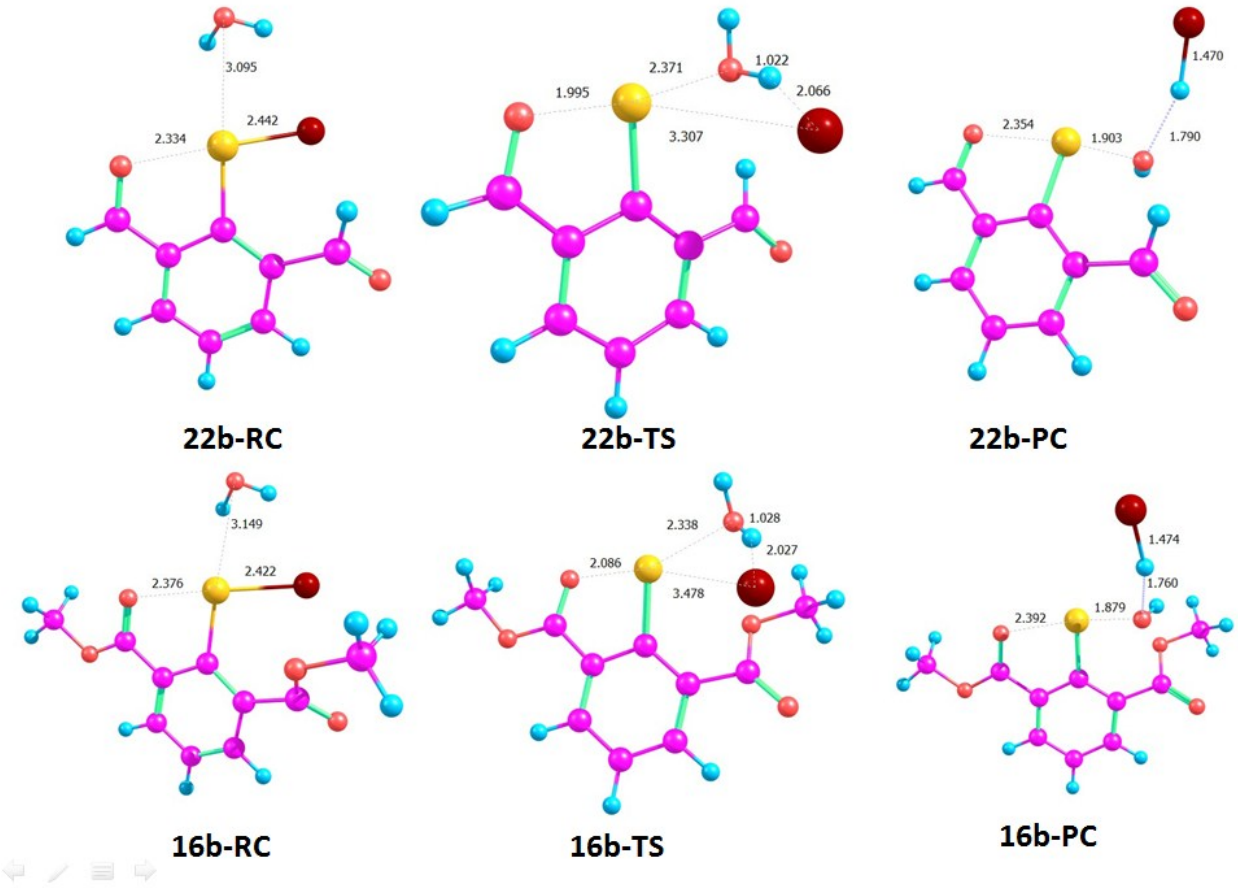

Table S5.

Entry	Sum of electronic and thermal Free Energies	$\Delta G^{\#}$ (kcal/mol)
22b-RC	-5505.724647	27.09
22b-TS	-5505.681470	
22b-PC	-5505.701324	
16b-RC	-5734.769893	32.239
16b-TS	-5734.718516	
16b-PC	-5734.745691	

S8. Dispersion contribution to E_{net} and E_{IChB}

The E_{net} values for the systems (**2b, 4b**, **8**, **36**, **37**, **9b**, **10b**, **16b**, **17b**, and **22b**) were computed using dispersion included (Grimme D2 and D3) and dispersion not included DFT methods at B3LYP/6-31G(d) level.[6] The correlation plots between E_{net} obtained using dispersion not included and included DFT methods are shown in Figure S3 and S4. The correlation plots between E_{IChB} for 2,6-disubstitued system is shown in figure S5. The computed E_{net} values are provided in Table S6.

Table S6. Table provides net stabilization energies (E_{net}) computed for the systems (**2b, 4b**, **8**, **36**, **37**, **9b**, **10b**, **16b**, **17b**, and **22b**) using dispersion not included and dispersion included DFT methods.

Entry	**B3LYP/6-31g(d) (kcal/mol)**	**DFT-D2 (kcal/mol)**	**DFT-D3 (kcal/mol)**	**%E_{Dis}***
2b	-3.38276	-3.34648	-3.4718	3
4b	-1.90577	-2.63366	-2.58639	26
8	-7.88995	-7.78618	-7.96924	0
36	-2.12671	-2.18456	-2.34819	9
37	-5.79342	-5.95793	-6.03724	4
9b	3.8076	2.31614	2.104189	45
10b	7.110189	4.221052	3.936324	45
16b	3.694356	1.068164	0.87494	76
17b	-2.57865	-5.58688	-5.03563	49
22b	-0.37532	-1.34294	-1.6939	78

***E_{dis} = E_{net}(DFT) – E_{net}(DFT-D3)**

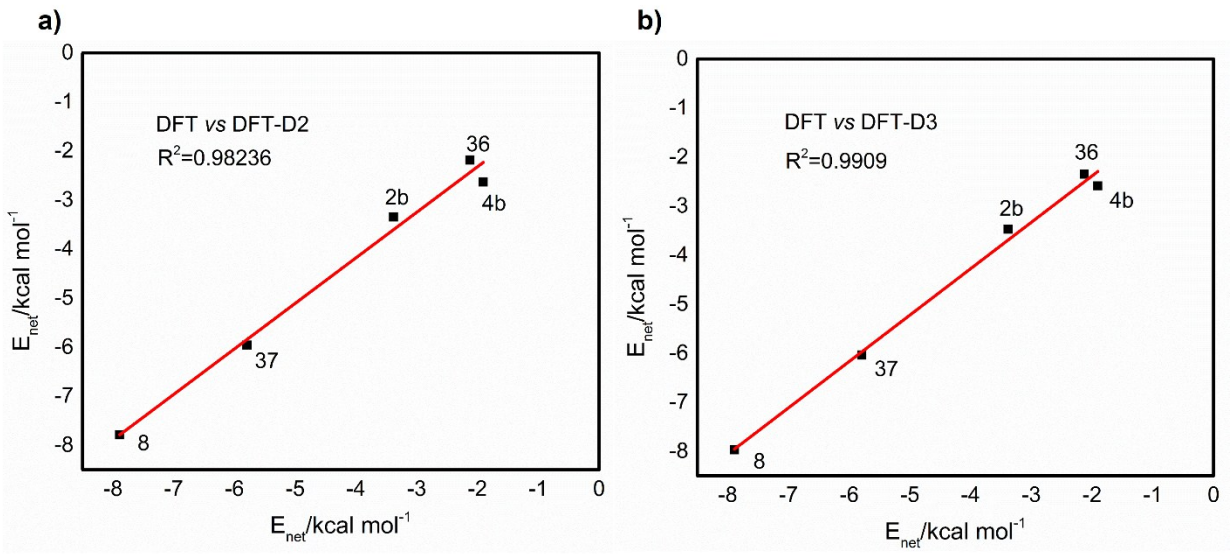

Figure S3. (a) The plot of E_{net} (DFT) Vs E_{net} (DFT-D2) for 2-substituted systems; (b) The plot of E_{net} (DFT) Vs E_{net} (DFT-D3) for 2-substituted systems

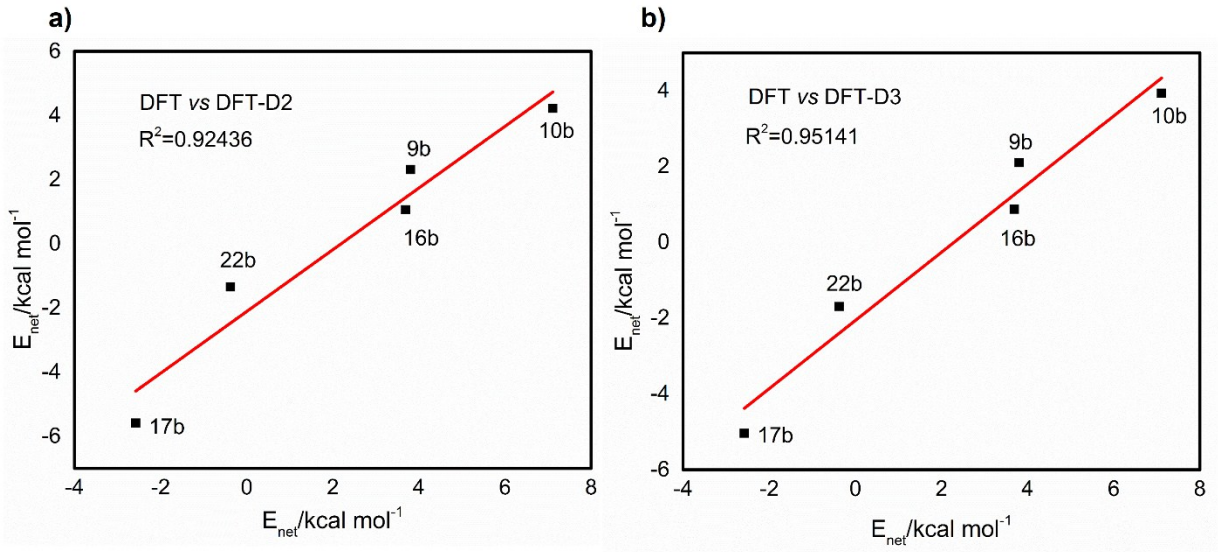

Figure S4. (a) The plot of E_{net} (DFT) Vs E_{net} (DFT-D2) for 2,6-substituted systems; (b) The plot of E_{net} (DFT) Vs E_{net} (DFT-D3) for 2,6-disubstituted systems

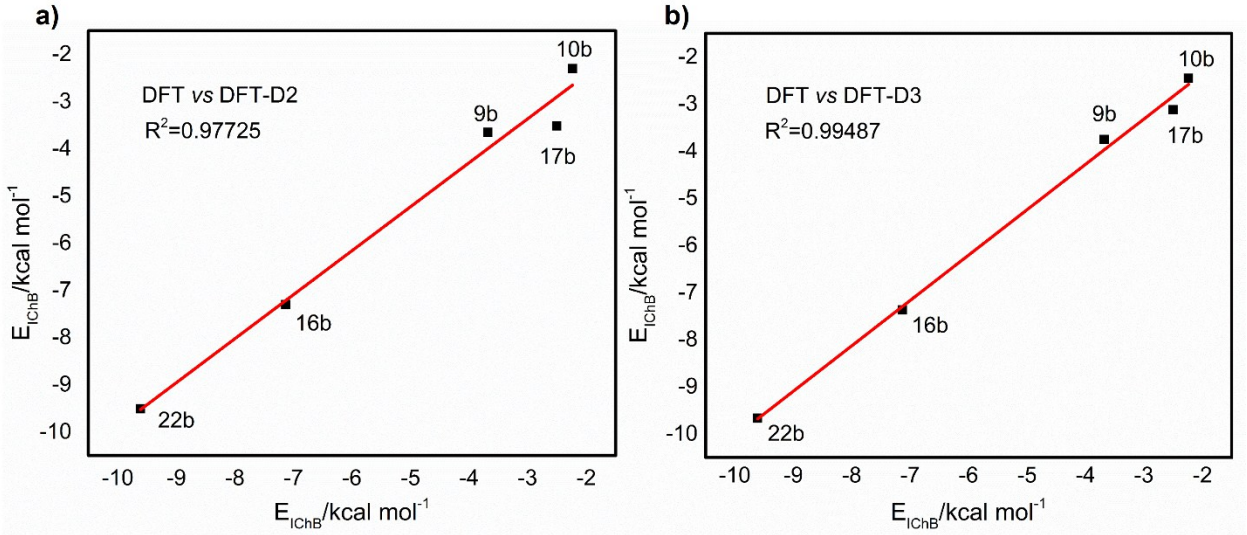

Figure S5. (a) The plot of E_{IChB} (DFT) Vs E_{IChB} (DFT-D2) for 2,6-substituted systems; (b)The plot of E_{IChB} (DFT) Vs E_{IChB} (DFT-D3) for 2,6-disubstituted systems.

S9. References

1. Chemcraft - graphical software for visualization of quantum chemistry computations. http://www.chemcraftprog.com

2. (a) Gaussian 09, Revision A.02, M. J. Frisch, G. W. Trucks, H. B. Schlegel, G. E. Scuseria, M. A. Robb, J. R. Cheeseman, G. Scalmani, V. Barone, B. Mennucci, G. A. Petersson, H. Nakatsuji, M. Caricato, X. Li, H. P. Hratchian, A. F. Izmaylov, J. Bloino, G. Zheng, J. L. Sonnenberg, M. Hada, M. Ehara, K. Toyota, R. Fukuda, J. Hasegawa, M. Ishida, T. Nakajima, Y. Honda, O. Kitao, H. Nakai, T. Vreven, J. A. Montgomery, Jr., J. E. Peralta, F. Ogliaro, M. Bearpark, J. J. Heyd, E. Brothers,
K. N. Kudin, V. N. Staroverov, R. Kobayashi, J. Normand, K. Raghavachari, A. Rendell, J. C. Burant, S. S. Iyengar, J. Tomasi, M. Cossi, N. Rega, J. M. Millam, M. Klene, J. E. Knox, J. B. Cross, V. Bakken, C. Adamo, J. Jaramillo, R. Gomperts, R. E. Stratmann, O. Yazyev, A. J. Austin, R. Cammi, C. Pomelli, J. W. Ochterski, R. L. Martin, K. Morokuma, V. G. Zakrzewski, G. A. Voth, P. Salvador, J. J. Dannenberg, S. Dapprich, A. D. Daniels, O. Farkas, J. B. Foresman, J. V. Ortiz, J. Cioslowski, and D. J. Fox, Gaussian, Inc., Wallingford CT, 2009.

3. a) R. F. W. Bader, Atoms in Molecules: A quantum Theory, Oxford University Press, New York, 1990; b) R. J. Gillespie and P. L. A. Popelier, Chemical Bonding and Molecular Geometry, Oxford University Press, New York, 2001.
(b) Gaussian 09, Revision D.01, M. J. Frisch, G. W. Trucks, H. B. Schlegel, G. E. Scuseria, M. A. Robb, J. R. Cheeseman, G. Scalmani, V. Barone, B. Mennucci, G. A. Petersson, H. Nakatsuji, M. Caricato, X. Li, H. P. Hratchian, A. F. Izmaylov, J. Bloino, G. Zheng, J. L. Sonnenberg, M. Hada, M. Ehara, K. Toyota, R. Fukuda, J. Hasegawa, M. Ishida, T. Nakajima, Y. Honda, O. Kitao, H. Nakai, T. Vreven, J. A. Montgomery, Jr., J. E. Peralta, F. Ogliaro, M. Bearpark, J. J. Heyd, E. Brothers, K. N. Kudin, V. N. Staroverov, T. Keith, R. Kobayashi, J. Normand, K. Raghavachari, A. Rendell, J. C. Burant, S. S. Iyengar, J. Tomasi, M. Cossi, N. Rega, J. M. Millam, M. Klene, J. E. Knox, J. B. Cross, V. Bakken, C. Adamo, J. Jaramillo, R. Gomperts, R. E. Stratmann, O. Yazyev, A. J. Austin, R. Cammi, C. Pomelli, J. W. Ochterski, R. L. Martin, K. Morokuma, V. G. Zakrzewski, G. A. Voth, P. Salvador, J. J. Dannenberg, S. Dapprich, A. D. Daniels, O. Farkas, J. B. Foresman, J. V. Ortiz, J. Cioslowski, and D. J. Fox, Gaussian, Inc., Wallingford CT, 2013.
4. T. Lu and F. Chen, *J. Mol. Graph. Model*., 2012, **38**, 314-323
5. Humphrey, W., Dalke, A. and Schulten, K., "VMD - Visual Molecular Dynamics", J. Molec. Graphics, 1996, **14**, 33-38.
6. (a) S. Grimme, *J. Comput. Chem*., 2006, **27**, 1787-1799; (b) S. Grimme, J. Antony, S. Ehrlich and H. Krieg, J. Chem. Phys., 2010, **132**, 154104; (c) F. De Vleeschouwer, M. Denayer, B. Pinter, P. Geerlings and F. De Proft. *J. Comput. Chem*. 2018, **39**, 557–572.